RESEARCH PAPER

The Improved Photocatalytic Performance of Strontium Titanate (STO) Powder Induced by Lanthanum Dopants

Yofentina Iriani[1],*, Novia Fajar Suryaning Puspita[1], Dianisa Khoirum Sandi[3], Fahru Nurosyid[1], Risa Suryana[1], Didier Fasquelle[2]

* *yofent_iriani@staff.uns.ac.id*

[1] Department of Physics, Faculty of Mathematics and Natural Science, Universitas Sebelas Maret, 57126, Indonesia
[2] Department of Unitede Dynamique et Structure des Materiaux Moleculaires, Universite du Littoral-Cote d'Opale, CS 80699F-62228 Calais, France
[3] Study Program of Energy Conversion Engineering, Department of Mechanical Engineering, Politeknik Negeri Semarang, 50275, Semarang, Indonesia

Abstract: *In this research, Lanthanum (La)-doped Strontium Titanate (STO) with the formula of $Sr_{1-x}La_xTiO_3$ (LSTO; x=0, 0.03, 0.05, and 0.07) powders have been successfully fabricated by co-precipitation route. The impacts of La^{3+} on the structural, microstructure, band-gap, and photocatalytic activity for the degradation of organic pollutants, in this case, methylene blue, under UV exposure, were reported in detail. The formation of undoped and La-doped STO samples with cubic perovskite structures was confirmed by X-ray Diffraction (XRD) results. The presence of La doping affected the microstructure morphology by producing LSTO powders with a larger specific surface area. Besides, the UV absorption of the LSTO powders was enhanced due to the narrowed band gap caused by La^{3+} dopants. Accordingly, an improvement in photocatalytic activity applied for the photodegradation of methylene blue solution was exhibited by the LSTO samples.*

Keywords: Lanthanum-doped strontium titanate, Photocatalyst, Photodegradation, Methylene blue.

Photodegradation process of methylene blue by Lanthanum-doped Strontium Titanate
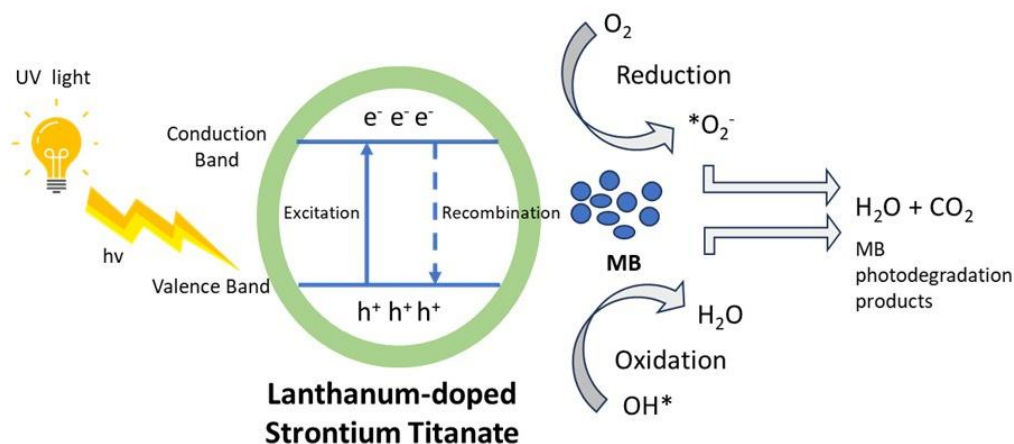
1. INTRODUCTION

Food, pharmacy, plastic, printing, and primarily garment factories cannot be separated from various dyes to color their products. With the increasing demand for the factories' production to color their products, the use of multiple dyes, including organic dyes, is increasing annually. The coloring activities from the factories generate vast amounts of wastewater, mainly composed of dyes. Unfortunately, because their nature is highly resistant to external influences, these dyes can hardly be removed and neutralized in the waters by conventional techniques such as filtration, chemical absorption, etc [1, 2]. It results in the prolonged accumulation of dye particles in wastewater that further dangers the water's environment and has mutational impacts on

1

flora and fauna—one of the organic dyes most extensively exploited in methylene blue (MB) factories [3, 4].

Economically and environmentally friendly techniques are required to treat wastewater. Photocatalysis is the cleanest technique that can be employed to degrade organic pollutants in wastewater into water with harmless substances [2, 5, 6]. The method occurs under light sources (UV, sunlight, microwave, etc) and requires a photocatalyst. During the process, the meeting of the two will release photogenerated charge carriers, which stimulate a chemical reaction with the wastewater, thereby releasing harmful chemicals that can then be removed [4, 7]. The existence of a photocatalyst has a critical role in the degradation of dye wastewater.

Among various candidates, strontium titanate (SrTiO$_3$ or STO) has recently become the promising photocatalyst material investigated for water splitting and organic compound degradation. STO is studied due to its remarkable properties, such as n-type semiconducting features, advantageous crystalline structure, tunable morphologies, and high stability [5, 8, 9]. Besides, STO has high efficiency, durable photostability, corrosion resistance, and suitable electrical properties. Unfortunately, the wide band gap of STO, about 3.2 eV, consequently causes it to only respond to UV light and a small amount of the solar spectrum [10-12]. This condition reduces the light absorption capability and furthers photocatalytic performance [5, 11]. Besides, the frequently used STO nanoparticles have a large specific surface area, making them easily agglomerate and challenging to recycle. Also, standard semiconductor photocatalysis processes involve photon absorption, band gap excitation, electron-hole pairs separation, and redox reactions at the photocatalyst surface [4, 13, 14]. Therefore, fixing this issue is extremely necessary to advance the photocatalytic performance of STO further.

In recent decades, many researchers have tried to improve STO's photocatalytic efficiency by engineering physicochemical properties. Numerous strategies have been employed, including the cocatalyst combination, nanostructure design, heterojunction construction, doping, etc. Still, doping has been the most frequently used strategy due to its simplicity and inexpensive process [8]. Naturally, doping transition metal ions into the STO lattice effectively induces a red shift in the band gap of STO and inhibits the recombination of photogenerated carriers.

Nb-doped STO has also been used to adjust the energy band of STO, demonstrating an improved photocatalytic performance for degrading methylene blue [5]. Afriani et al. have prepared Mn-doped STO, which showed improved MB photodegradation due to Mn doping, indicating increased photocatalytic activity [7]. The morphology and microstructure of V-doped STO photocatalysts were studied, revealing excellent photocatalytic activity [12]. Eu-doped STO has also been fabricated, revealing that Eu doping could increase the specific surface area, decrease the band gap, and further enhance the photocatalytic performance for methyl orange removal [15]. Another work reported the fabrication of 15 types of rare earth ions doped STO and the dopants' impact on the morphology, optical properties, and photocatalytic activity for the photodegradation of rhodamine B (RhB) exhibiting an enhancement [8]. N-doped STO has also been utilized as a photocatalyst for degrading methyl orange, showing an increase in the photocatalytic performance compared to STO due to the narrowed band gap [16]. Other studies have also reported the doping of nickel (Ni), neodymium (Nd), and aluminum (Al) in STO, as well as the study of photocatalytic performance [17-19].

Among the doping elements, Lanthanum (La) becomes one of the most crucial dopants from the transition metals chosen since La^{3+} (r= 1.15 Å) has a nearly closed ionic radius to Sr^{2+} (r= 1.13 Å) [20, 21]. Besides, both have identical coordination numbers of 6, which prevents significant lattice strain when La^{3+} is substituted into the Sr^{2+} ion in the STO host structure [21-23]. Furthermore, it has been reported that La doping enhances the surface area, pore volume, and adsorption capacity and prevents electron-hole recombination, improving STO's photocatalytic performance [10, 13].

To the best of our knowledge, works on the preparation and characterization of lanthanum-doped STO and its photocatalytic activity for methylene blue photodegradation remain scarce. Therefore, this study synthesized the pure and lanthanum-doped STO photocatalysts using the co-precipitation route. The influences of La doping on the structural, morphological, and

2

optical properties and photocatalytic activity against the degradation of MB were investigated. The findings would be helpful for further studies on photocatalyst properties.

2. EXPERIMENTAL PROCEDURES

2.1. Sample Preparation

The materials were strontium nitrate $(Sr(NO_3)_2)$ (Sigma-Aldrich, 95%), oxalic acid $(C_2H_2O_4)$ (Sigma-Aldrich, >99%), titanium tetrabutoxide $(Ti(C_4H_9O)_4)$ (Sigma-Aldrich, 97%), isopropanol $((CH_3)_2CHOH)$ (Sigma-Aldrich, >99%), lanthanum nitrate hexahydrate $(La(NO_3)_3.6H_2O)$ (Sigma-Aldrich, >99%), distilled water, ethanol (Sigma-Aldrich, >99%), and methylene blue.

La-doped STO samples were made by mixing ammonium oxalate dissolved in isopropanol and stirred with a magnetic stirrer for 45 min. The titanium tetrabutoxide solution was poured into the ammonium oxalate solution and stirred with a magnetic stirrer for 30 min. Lanthanum nitrate hexahydrate powder (this material was absent for the STO sample), strontium nitrate, and isopropanol were added to the solution and stirred using a magnetic stirrer for 45 min. The final solution was titrated with distilled water and then deposited for 24 hours. After that, the solution was then filtered, leaving precipitates, and washed with ethanol once and distilled water twice until reaching a pH of about 7. The precipitate was filtered and then hydrolyzed at 100°C for 10 hours to obtain powder. The powder was then sintered at 1000°C for 4 hours. The samples were later called STO, LSTO3, LSTO5, and LSTO7 for La dopant concentration (x) of 0, 0.03, 0.05, and 0.07, respectively.

2.2. Characterization

The structural property of the photocatalysts was observed via powder X-ray diffractometer (Bruker D8 Advanced) using Cu-Kα ray with wavelength λ= 1.541 Å. XRD patterns were extracted and employed to calculate the lattice constant and crystallite size. The crystallite size was calculated using the Debyer-Scherrer method (Eq. 1). The surface area was observed by N_2 adsorption-desorption isotherms on an automated gas adsorption analyzer (Quantachrome Instrument, USA) at 77 K using the Brunauer-Emmett-Teller (BET) procedure. Further, the specific surface area was obtained by dividing the surface area by

the tested sample mass. The optical property, in this case, the absorbance and band gap energy, was examined from a UV-visible diffuse reflectance spectrum (UV-Vis DRS) by a Shimadzu MPC-2200 spectrophotometer. The scan range was 200 to 700 nm, and the scan rate was 20 nm/min. The band gap energy (E_g) of the photocatalysts was estimated by applying the Kubelka-Munk and the Tauc plot functions as Eqs. 2-3 [3, 12].

$$D = \frac{k\lambda}{\beta \cos \theta} \tag{1}$$

Where β represents the FWHM value (rad), θ is the X-ray diffraction angle (degrees), k is Scherrer's constant (0.94), and λ is Cu wavelength (nm).

$$F(R) = \frac{(1-R)^2}{2R} \tag{2}$$

$$F(R)h\nu = A(h\nu - E_g)^n \tag{3}$$

Where R is the reflectance and F(R) and the Kubelka-Munk function. A is the absorbance, h is the Planck constant, and n is ½ and 2 for direct and indirect transitions, respectively.

2.3. Photocatalytic Performance of STO and LSTO

The photocatalytic activity was tested using methylene blue dye under UV light exposure with a 200-300 nm wavelength. The photocatalyst (0.1 g) was uniformly dispersed in the methylene blue solution (1 ppm) and then was left for 30 min in a dark condition to obtain adsorption-desorption before irradiation. 3 mL of solution was sampled and centrifuged for 30 min to extract the photocatalyst powder. The solution was then exposed to UV light for 1, 3, and 5 hours. The irradiated solution at certain exposure times was then observed with a UV-Vis Spectrophotometer exhibiting absorbance spectra. The absorbance values were then used to compute the percentage of methylene blue degradation via Eq. 4.

$$\%degradation = \frac{A_o - A_t}{A_o} x100\% \tag{4}$$

3. RESULTS AND DISCUSSION

3.1. Structural Property

Fig. 1 presents the XRD diffractograms of the STO and LSTO samples. All peaks of the diffractograms were attributed to the phase of STO with cubic perovskite structure (JCPDS no. 73-0661). Weak peaks at about 25.20° and 27.43° were detected in STO, LSTO3, and LSTO5 samples.

Fig. 1. a) XRD patterns, b) crystallite size, and c) lattice constant of STO and LSTO samples

The peaks corresponded to the existence of a slight impurity of $SrCO_3$ (JCPDS no. 74-1491). The impurity was induced by the carbon sources from the materials during the fabrication, such as ethanol, since $SrCO_3$ hardly vanishes under air circumstances during the fabrication [21].

The sharp peaks in the XRD diffractograms denote that the samples fabricated by the co-precipitation route were highly crystalline [24].

Fig.s 1b and 1c depict the estimated lattice constants and crystallite sizes, respectively. According to Fig. 1b, the lattice constants of STO, LSTO3, LSTO5, and LSTO7 samples were 3.9066, 3.9088, 3.9076, and 3.9081 Å, respectively. An increase in lattice constants in LSTO samples compared to that of STO was observed due to the interstitial insertion of La ions in the Sr positions in the STO lattice. It is considered because La^{3+} possesses a larger ionic radius (0.115 nm) than Sr^{2+} (0.113 nm) [20]. The average crystallite sizes were computed by the Debyer-Scherrer method, and the values were 37.9, 37.8, 35.4, and 37.5 nm for STO, LSTO3, LSTO5, and LSTO7, respectively. It reveals that the crystallite size values were reduced due to the La doping, meaning that the introduction of La in the STO lattice can inhibit crystal growth.

Fig. 2 displays the FTIR spectra of STO and LSTO photocatalysts.

The broad absorption bands at about 3429 cm^{-1} and the bands at around 3724 cm^{-1} and 1624 cm^{-1} denote the stretching and bending vibrations of the O—H bonds [24, 25]. The presence of the bonds originates from H_2O molecules, indicating that the samples could absorb a small amount of water molecules or bond some hydroxyl groups [24]. The absorption peaks at about 1460 cm^{-1} are attributed to the O=C-O carboxyl [26]. It can be correlated to carbonate species denoting the emergence of $SrCO_3$, which aligns with the XRD spectra [26, 27]. The adsorption peaks below 1000 cm^{-1} at 857 cm^{-1} are attributed to TiO_6 octahedron vibration, and the prominent ones at 550 to 700 cm^{-1} are assigned to the $SrTiO_3$ crystal

4

lattice vibrations [13, 26].

Fig. 2. FTIR spectra of samples

3.2. Optical Property

Diffuse-reflectance UV-Vis absorption spectra, as presented in Fig. 4a, were applied to investigate the light absorption ability of LSTO photocatalysts by observing the absorption edge and energy gap [13, 16]. According to Fig. 4a, the absorption edge of LSTO samples tends to move toward longer wavelength directions, mainly LSTO5. It indicates increased light absorption and enhancement in photocatalytic activity [4, 16].

The band gap values of STO and LSTO were determined by fitting the optical transition at the absorption edges using the Kubelka-Munk and Tauc plot function (Fig. 3b). The band gap of STO was estimated to be 3.24 eV, which is appropriate to that reported by Aravinthkumar et al. [24]. Meanwhile, the band gaps of LSTO3, LSTO5, and LSTO7 were computed to be 3.12, 3.02, and 3.15 eV, respectively. This implies that the la doping in the STO lattice caused the narrowed band gap. A theoretical study conveyed that the La atoms can raise the conduction band due to the hybridization of La 3d and Ti 3d, leading to a narrower band gap [22]. In particular, the least band gap energy was achieved by LSTO5.
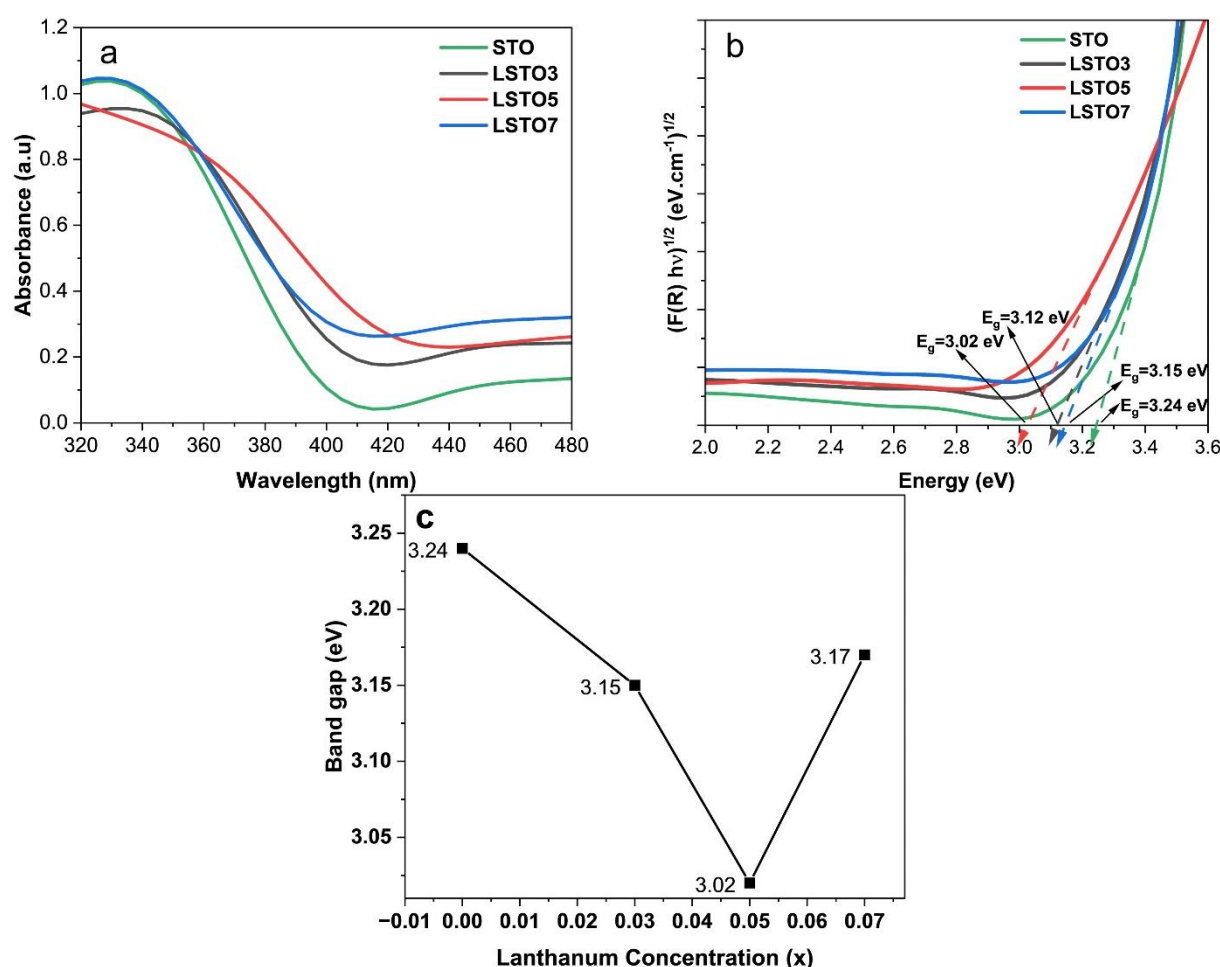

Fig. 3. a) Absorbance spectra, b) Kubelka Munk plots of the photocatalysts, and c) band gap energy

Fig. 4. Specific surface area of the photocatalysts. The inset is a nitrogen adsorption-desorption isotherm curve of LSTO5

A smaller band gap means a reduced amount of energy is needed for electronic transitions to react, thereby facilitating the photocatalysis process [15, 28].

3.3. Microstructure

Fig. 4 presents the BET-specific surface area of the STO and LSTO samples. The specific surface area of the STO sample was 113 m^2/g, and the values enlarged at 123 and 234 m^2/g for LSTO3 and LSTO5, respectively. The results indicate that LSTO powders demonstrated a larger surface area than pure STO. This occurrence should be attributed to the reduced crystallite sizes compared to STO [22]. The shrinkage crystallite size indicates the more area occupied by the crystal, like quantum dots, resulting in a higher surface area. Similar to prior research, the specific surface area of LSTO enlarged with higher La doping [22]. The larger surface area is advantageous for the utilization of light sources, which allows more reaction sites and reinforces the light absorption intensity, leading to increased photocatalytic activity [24, 29]. As for LSTO7, the specific surface area turned to drop by 109 m^2/g. This phenomenon is probably because excessive doping, in this case x= 0.07, promotes agglomeration, which can reduce the specific surface area [30]. These results follow previous research, where a suitable amount of metal doping can increase the surface area. Still, if the doping is excessive, it turns to reduce the surface area [5]. The inset graph of Fig. 3 displays the N_2 adsorption-desorption isotherm of a characteristic LSTO5 sample. It denotes physisorption isotherms

exhibiting a hysteresis loop under type IV based on the IUPAC reference, implying that the sample is considered mesoporous [10, 12]. The result was similar to the La-doped STO synthesized by the sol-gel method [13]. Similar results were obtained from other LSTO samples and pure STO.

3.4. Photocatalytic Performance

The photocatalytic activity of the STO and LSTO photocatalysts was tested by degrading methylene blue under UV exposure. Fig. 5a demonstrates the %degradation of methylene blue with STO and LSTO photocatalysts gradually increasing with exposure times. Besides, the picture also exhibits that the %degradation of methylene blue by LSTO samples was higher than that of STO (with La concentration increases). Table 1 presents the %degradation of methylene blue by all photocatalysts. The %degradation of methylene blue by LSTO3, LSTO5, and LSTO7 after 5-hour irradiation was 74, 77, and 68, respectively, which was insignificantly different. After 5 hours, the %degradation of the STO (x= 0) sample was 42%. This value was better compared to STO produced by the sol-gel technique, revealing 36% MB dye degradation after 8 h UV irradiation[13].

In this study, the highest degradation was demonstrated by LSTO5 about 77%, denoting the optimal photocatalytic reaction. Here, La doping more than x= 0.05 was ineffective for %degradation. These yields are comparable with prior results. For instance, the La-doped STO (La concentration, x= 0.5) made by the sol-gel technique was used to degrade methylene blue under UV, showing a degradation of about 20% in 5 hours [13]. Also, co-doped STO (La 5% and Fe 2%) synthesized with the solid-state reaction method exhibited 76% methyl orange degradation under visible light treatment for 3 hours [10].

The insertion of lanthanum ions into the STO lattice could inhibit crystal growth, increase the surface area, reduce the band gap, and help the strong adsorption of the reactants on the photocatalyst surfaces. These aspects have a significant impact on improved photocatalytic activity. The higher specific surface area indicates that more pollutants can be adsorbed onto the surface of the photocatalyst, providing more accessible areas for electron-hole pair separation and increasing the possibility of photodegradation [1, 6, 15, 31]. Thus, it is acceptable if the LSTO5 exhibits the highest photodegradation efficiency

6

since it possesses the largest specific surface area.

Still, if viewed from the trend, the efficient photocatalytic response might be due to the lower band gap energies of LSTO compared to pure STO. La doping resulted in a narrow band gap (i.e., 3.12, 3.02, and 3.15 for LSTO3, LSTO5, and LSTO7, respectively). The band gap energy has a significant influence on the photocatalytic performance. The narrow band gap leads to efficient UV light absorption, effective electron-hole pairs photogeneration, and rapid charge carrier recombination inhibition, thereby promoting photocatalytic degradation [1, 15, 30].

The photodegradation kinetics of methylene blue was measured, and it fitted the typical pseudo-first-order as Eq. 5 [1, 30]. Where k represents the kinetic rates. The pseudo-first-order is a linear relationship between $\ln C_t/C_o$ and time (t).

$$\ln {}^{C_t}/_{C_o} = -kt \tag{5}$$

Table 1 displays the kinetic rates for the degradation of methylene blue dye by STO and LSTO photocatalysts. The values for LSTO photocatalysts also improved compared to pure STO due to La doping. The highest activity revealing the highest kinetic rate of 0.00446/min was exhibited by LSTO5, corresponding to the highest photocatalytic activity against methylene blue dye.

Fig. 5. a) Degradation percentage of methylene blue exposed under the UV light b) Pseudo-first order kinetics of the methylene blue photocatalytic degradation, and c) Time-dependent UV–Vis spectra of degraded methylene blue solution by LSTO7

Table 1. Photocatalytic degradation of MB by photocatalysts under UV light

Photocatalysts	% methylene blue degradation at 5 h	Kinetic constant (k, min⁻¹)	Relative coefficient (R²)
STO	42	0.00144	0.8372
LSTO3	74	0.00427	0.9771
LSTO5	77	0.00446	0.9428
LSTO7	68	0.00387	0.9974

7

Hence, it is evident that the narrow band gap of the photocatalysts causes a monotonic increase in the kinetic rate [1]. Fig. 5c presents the absorbance peak (λ_{max}) of methylene blue at diverse exposure times at 664 nm from the LSTO7. After an exposure time of 5 h, the λ_{max} of methylene blue continuously declined due to decolorization of the methylene blue. Further, the spectra absorbance of STO and each LSTO sample also demonstrate the same trends.

The fundamental process of photocatalytic activity can be explained in Fig. 6 [1, 13, 24, 31]. When the photocatalysts are exposed to photons having energy greater than or equal to their band gap, the electrons from the photocatalysts will be excited. Then, the photoexcited electrons quickly jump from the valence band to the conduction band of STO, producing holes. Then, these photogenerated charge carriers travel to the surface of the photocatalysts to stimulate redox reactions. The electrons react with oxygen to yield superoxide radicals ($*O_2^-$) while holes react with the water molecules to generate hydroxyl radicals (OH*). Meanwhile, reactions of the superoxide anions ($*O_2^-$) with water yield hydrogen peroxide (H_2O_2) molecules, which decay into hydroxyl radicals (OH*) in the incidence of light. These exceedingly active radicals (OH* and $*O_2^-$) respond with methylene blue and decay to carbon dioxide and water without any byproducts.

4. CONCLUSION

La-doped STO samples were fabricated by the co-precipitation route, and the improvement of the photocatalytic activity of La-doped STO photocatalysts was demonstrated. The La ions doping in the STO lattice could inhibit crystal growth and enlarge the specific surface area. This might give more available active sites for electron-hole pair separation and thereby improve photodegradation possibility. In addition, La doping narrowed the band gap of STO, increasing UV light absorption capability. As a result, the La-doped STO photocatalysts demonstrated a significant improvement in photocatalytic activity than pure STO.

ACKNOWLEDGMENTS

REFERENCES

[1].   Khatun, M., Mitra, P., and Mukherjee, S., "Effect of Band Gap and Particle Size on Photocatalytic Degradation of NiSnO₃ Nanopowder for Some Conventional Organic Dyes." Hybrid Advances., 2023., 4, 1-9.

[2].   Jaramillo-Fierro, X., Cuenca, G., and Ramon, J., "The Effect of La$^{(3+)}$ on the Methylene Blue Dye Removal Capacity of the La/ZnTiO$_{(3)}$ Photocatalyst, a DFT Study." Nanomaterials., 2022, 12 (18). 1-21.

[3].   Zdorovets, M. V., Borgekov, D. B., Zhumatayeva, I. Z., Kenzhina, I. E., and Kozlovskiy, A. L., "Synthesis, Properties and Photocatalytic Activity of CaTiO$_{(3)}$-Based Ceramics Doped with Lanthanum." Nanomaterials., 2022, 12 (13), 2241.

Fig. 6. Fundamental process of methylene blue photodegradation by LSTO samples

[4]. Alomair, N. A., "The Role of Strontium on The Enhancement of Photocatalytic Response of TiO2 Nanotubes–Application in Methylene Blue and Formic Acid Photodegradation Under Visible Light and UV-A." Arab. J. Basic Appl. Sci., 2022, 29 (1), 162-174.

[5]. Nunocha, P., Kaewpanha, M., Bongkarn, T., Eiad-Ua, A., and Suriwong, T., "Effect of Nb doping on The Structural, Optical, and Photocatalytic Properties of SrTiO$_3$ Nanopowder Synthesized by Sol-Gel Auto Combustion Technique." J. Asian Ceram. Soc., 2022, 10 (3), 583-596.

[6]. Mohtar, S. S., Aziz, F., Ismail, A. F., Sambudi, N. S., Abdullah, H., Rosli, A. N., and Ohtani, B., "Impact of Doping and Additive Applications on Photocatalyst Textural Properties in Removing Organic Pollutants: A Review." Catalysts., 2021, 11 (10), 1-30.

[7]. Iriani, Y., Afriani, R., Sandi, D. K., and Nurosyid, F., "Co-precipitation Synthesis and Photocatalytic Activity of Mndoped SrTiO3 for the Degradation of Methylene Blue Wastewater." Evergreen., 2022, 09 (04), 1039-1045.

[8]. Song, Y.-X., Ma, W.-Q., Chen, J.-J., Xu, J., Mao, Z.-Y., Wang, D.-J., "Photocatalytic Activity of Perovskite SrTiO$_3$ Catalysts Doped with Variable Rare Earth Ions." Rare Met., 2021, 40 (5), 1077-1085.

[9]. Kumar, M., Basera, P., Saini, S., and Bhattacharya, S., "Role of Defects in Photocatalytic Water Splitting: Monodoped vs Codoped SrTiO$_3$." J. Phys. Chem. C., 2020, 124 (19), 10272-10279.

[10]. Abdi, M., Mahdikhah, V., and Sheibani, S., "Visible Light Photocatalytic Performance of La-Fe co-Doped SrTiO$_3$ Perovskite Powder." Opt. Mater., 2020, 102, 109803.

[11]. Adeyemi, A. N., Venkatesh, A., Xiao, C., Zhao, Z., Li, Y., Cox, T., Jing, D., Rossini, A. J., Osterloh, F. E., and Zaikina, J. V., "Synthesis of SrTiO$_3$ and Al-doped SrTiO$_3$ via the Deep Eutectic Solvent Route." Mater. Adv., 2022, 3 (11), 4736-4747.

[12]. Bantawal, H., Shenoy, U. S., and Bhat, D. K., "Vanadium-Doped SrTiO$_3$ Nanocubes: Insight Into Role of Vanadium in Improving the Photocatalytic Activity." Appl. Surf. Sci., 2020, 513, 145858.

[13]. Nunocha, P., Kaewpanha, M., Bongkarn, T., Phuruangrat, A., and Suriwong, T., "A New Route to Synthesizing La-doped SrTiO$_3$ Nanoparticles Using the Sol-Gel Auto Combustion Method and Their Characterization and Photocatalytic Application." Mater. Sci. Semicond. Process., 2021, 134, 106001.

[14]. Galloni, M. G., Cerrato, G., Giordana, A., Falletta, E., and Bianchi, C. L., "Sustainable Solar Light Photodegradation of Diclofenac by Nano- and Micro-Sized SrTiO$_3$." Catalysts., 2022, 12 (8), 1-17.

[15]. Wang, Y., Ma, W., Song, Y., Chen, J., Xu, J., Wang, D., and Mao, Z., "Enhanced Photocatalytic Performance of SrTiO$_3$ Powder Induced by Europium Dopants." J. Rare Earths., 2021, 39 (5), 541-547.

[16]. Atkinson, I., Parvulescu, V., Pandele Cusu, J., Anghel, E. M., Voicescu, M., Culita, D., Somacescu, S., Munteanu, C., Šćepanović, M., Popovic, Z. V., and Fruth, V., "Influence of Preparation Method and Nitrogen (N) Doping on Properties and Photo-Catalytic Activity of Mesoporous SrTiO$_3$." J. Photochem. Photobiol. A., 2019, 368, 41-51.

[17]. Iriani, Y., Sandi, D. K., Hikmah, D. N., Afriani, R., Nurosyid, F., Handoko, E., and Faquelle, D., "Comparison Study of Aluminum (Al)-Doped Strontium Titanate (SrAl$_x$Ti$_{1-x}$O$_3$; x= 3% and 5%) Photocatalyst for Methylene Blue Degradation." Mater. Today: Proc., 2024.

[18]. Agustina, F. R., Suherman, B., Uswatun Hasanah, L., Fajar Suryaning Puspita, N., Khoirum Sandi, D., Nurosyid, F., Handoko, E., and Iriani, Y., "Preparation of Nickel (Ni) Doped SrTiO$_3$ and Effects of Sintering Temperatures on its Properties as Photocatalyst." J. Phys. Conf. Ser., 2023, 2498 (1), 012018.

[19]. Hasanah, L. U., Agustina, F. R., Puspita, N. F. S., Suherman, B., Nurosyid, F., Sandi, D. K., and Iriani, Y., "Microstructure, Chemical Bonds, and Photocatalyst Activity of Neodymium-Doped Strontium Titanate (Sr$_{0.97}$Nd$_{0.03}$TiO$_3$) with 900°C and 1000°C Sintering Temperature." J. Phys. Conf. Ser., 2022, 2392 (1), 012034.

[20]. Kaewdee, P., Limpichaipanit, A., Randorn, C., and Tandorn, S., "Facile and Composition

Controllable Synthesis of Lanthanum-Doped Strontium Titanate via Peroxide Route." Adv. Appl. Ceram., 2023, 122 (1), 17-21.

[21]. Ahmed, A. J., Nazrul Islam, S. M. K., Hossain, R., Kim, J., Kim, M., Billah, M., Hossain, M. S. A., Yamauchi, Y., Wang, X., "Enhancement of Thermoelectric Properties of La-doped $SrTiO_3$ Bulk by Introducing Nanoscale Porosity." Royal Soc. Open Sci., 2019, 6 (10), 190870.

[22]. Yang, D., Zou, X., Sun, Y., Tong, Z., and Jiang, Z., "Fabrication of Three-Dimensional Porous La-Doped $SrTiO_3$ Microspheres with Enhanced Visible Light Catalytic Activity for Cr(VI) Reduction." Front Chem Sci Eng., 2018, 12 (3), 440-449.

[23]. Deshmukh, V. V., Nagaswarupa, H. P., Ravikumar, C. R., Anil Kumar, M. R., Shashi Shekhar, T. R., and Ananda Murthy, H. C., "Lanthanum Doped Strontium Titanate Nanomaterial for Photocatalytic and Supercapacitor Applications." Asian J. Chem., 2020, 32 (8), 2013-2020.

[24]. Aravinthkumar, K., Praveen, E., Jacquline Regina Mary, A., and Raja Mohan, C., "Investigation on $SrTiO_3$ Nanoparticles as a Photocatalyst for Enhanced Photocatalytic Activity and Photovoltaic Applications." Inorg. Chem. Commun., 2022, 140, 109451.

[25]. Putri, Y. E., Faradilla, H., Satria, and D., Wellia, D. V., "Facile Synthesis of Lanthanum-Doped $SrTiO_3$ Nanocubes Mediated by Cetyltrimethylammonium Bromide and Tert-Butylamine Under Solvothermal Condition and Their Tunable Electrical Properties." Chim. Techno Acta., 2023, 10 (4), 202310407.

[26]. Wu, X., Wang, C., Wei, Y., Xiong, J., Zhao, Y., Zhao, Z., Liu, J., and Li, J., "Multifunctional Photocatalysts of Pt-Decorated 3DOM Perovskite-Type $SrTiO_3$ with Enhanced CO_2 Adsorption and Photoelectron Enrichment for Selective CO_2 Reduction with H_2O to CH_4." J. Catal., 2019, 377, 309-321.

[27]. Yang, S.-F., Niu, C.-G., Huang, D.-W., Zhang, H., Liang, C., and Zeng, G.-M., "$SrTiO_3$ Nanocubes Decorated with Ag/AgCl Nanoparticles as Photocatalysts with Enhanced Visible-Light Photocatalytic Activity Towards the Degradation of Dyes, Phenol and Bisphenol A." Environ. Sci. Nano., 2017, 4 (3), 585-595.

[28]. Chen, M., Xiong, Q., Liu, Z., Qiu, K., and Xiao, X., "Synthesis and Photocatalytic Activity of Na^+ Co-Doped $CaTiO_3$:Eu^{3+} Photocatalysts for Methylene Blue Degradation." Ceram. Int., 2020, 46 (8), 12111-12119.

[29]. Zhu, X., Pei, L., Zhu, R., Jiao, Y., Tang, R., and Feng, W., "Preparation and Characterization of Sn/La Co-Doped TiO(2) Nanomaterials and Their Phase Transformation and Photocatalytic Activity." Sci. Rep., 2018, 8 (1), 12387.

[30]. Matussin, S. N., Khan, F., Harunsani, M. H., Kim, Y. M., and Khan, M. M., "Photocatalytic Degradation of Brilliant Green and 4-Nitrophenol Using Ni-Doped Gd(OH)3 Nanorods." Sci. Rep., 2024, 14 (1), 8269.

[31]. Mehra, S., Saroha, J., Rani, E., Sharma, V., Goswami, L., Gupta, G., Srivastava, A. K., and Sharma, S. N., "Development of Visible Light-Driven $SrTiO_3$ Photocatalysts for the Degradation of Organic Pollutants for Waste-Water Treatment: Contrasting Behavior of MB & MO Dyes." Opt. Mater., 2023, 136, 113344.